

Temperature dependence for the photovoltaic device parameters of polymer-fullerene solar cells under operating conditions

E. A. Katz,^{a)} D. Faiman, and S. M. Tuladhar

Department of Solar Energy and Environmental Physics, Jacob Blaustein Institute for Desert Research, Ben-Gurion University of the Negev, Sede Boqer Campus, 84990, Israel

J. M. Kroon and M. M. Wienk

ECN Solar Energy, P.O. Box 1, 1755 ZG Petten, The Netherlands

T. Fromherz and F. Padinger

Quantum Solar Energy Linz (QSEL), Guberstrasse 40-42, A-4020 Linz, Austria

C. J. Brabec^{b)} and N. S. Sariciftci

Linz Institute for Organic Solar Cells (LIOS), Physical Chemistry, Johannes Kepler University Linz, Altenbergerstrasse 69, A-4040 Linz, Austria

(Received 1 June 2001; accepted for publication 14 August 2001)

We report on the temperature dependence of various photovoltaic device parameters of solar cells, fabricated from interpenetrating networks of conjugated polymers with fullerenes, in the wide temperature range of their possible operating conditions (25–60 °C). The open-circuit voltage was found to decrease linearly with increasing temperature. For the short-circuit current, we observed a monotonic increase with increasing temperature, followed by a saturation region. The rate of this increase (coupled to a corresponding increase for the fill factor) was found to overtake the corresponding rate of decrease in voltage, resulting in an overall increase of the energy conversion efficiency. The efficiency was observed to reach a maximum value in the approximate range 47–60 °C. The results are discussed with respect to possible mechanisms for photovoltage generation and charge carrier transport in the conjugated polymer-fullerene composite, and in particular, thermally activated charge carrier mobility. © 2001 American Institute of Physics.

[DOI: 10.1063/1.1412270]

I. INTRODUCTION

Organic solar cells, as alternatives to conventional inorganic photovoltaic devices, have a number of potential advantages, such as lightweight, flexibility, and low cost fabrication of large areas.^{1–8} One variety of organic solar cells that has recently been studied extensively consists of donor–acceptor heterojunctions between conjugated polymers and fullerenes (or fullerene derivatives).^{9–12} The efficient photoresponse of these polymer devices originates from an ultrafast photoinduced electron transfer from the conjugated polymer to the fullerene molecule.^{13–15} The kinetics of this process have recently been time resolved to occur within 40 fs.¹⁶ Since this is faster than any other relaxation mechanism in the conjugated polymer, the quantum efficiency of this process is estimated to be close to unity. The best photovoltaic parameters reported to date and in particular, energy conversion efficiencies of 2.5%,¹⁷ were for devices based on interpenetrating networks of conjugated polymers with fullerenes.

Due to the novelty of such devices, published information on the temperature dependence of the photovoltaic parameters of these solar cells in particular, and organic solar cells in general, is very limited. The significance of such

knowledge is twofold: fundamental and practical. At the fundamental level such information, particularly for organic solar cells, may provide insights into the mechanisms governing photovoltage generation and charge collection, as will be discussed in greater detail below.

At the practical level there is a twofold importance: Such information enables one to optimize the operation of such cells but no less important, it helps one to quantify cell performance in a manner that may be compared from one laboratory to another. In the case of conventional inorganic solar cells a set of standard test conditions (STC) have been defined. These correspond to a radiant intensity of 1000 W/m² with a spectral distribution defined as “AM1.5G” (IEC 904-3) and a cell temperature of 25 °C. In spite of the existence of such a standard, all kinds of efficiencies have been reported for organic solar cells, based on measurements performed under a large variety of test conditions.¹⁸

This article reports the results of accurate measurements performed both indoors (under appropriately corrected simulated STC conditions) and outdoors (under correspondingly corrected naturally occurring STC conditions). A detailed study of the resulting temperature dependence for these solar cells, based on interpenetrating networks of conjugated polymers with fullerenes, is presented. This enables us to discuss possible physical mechanisms which might be responsible for the observed temperature dependence.

^{a)}Electronic mail: keugene@bgumail.bgu.ac.il

^{b)}Present address: Siemens AG/CT MM1, Innovative Electronics, Paul-Gossenstr. 100, D 91052 Erlangen, Germany.

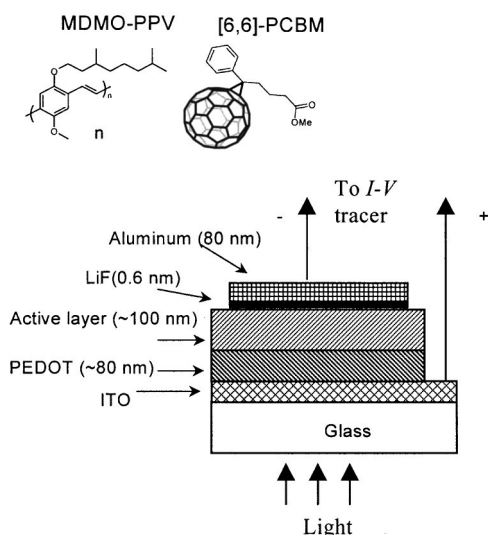


FIG. 1. Schematic device structure of conjugated polymer-fullerene solar cells under study, together with chemical structure of compounds used for the active layer.

II. EXPERIMENTAL TECHNIQUES

The underlying logistics for the experiments reported here were as follows. The solar cells were produced in Linz and given their first approximate characterization using a filtered metal-halide solar simulator (Steuernagel "Solar Constant 575," with calculated spectral mismatch factor $M = 0.76$).¹⁷ Samples were then sent to Petten for accurate indoor studies using a class-A xenon-arc solar simulator (Spectrolab XT-10, with calculated mismatch factor $M = 0.90$), and to Sede Boqer for accurate outdoor studies using the well-known AM1.5G natural spectrum of this site.^{19,20}

The bulk donor-acceptor heterojunction solar cells were produced by spin casting. The production process is described in detail elsewhere.^{11,17} Poly [2-methoxy, 5-(3',7'-dimethyl-octyloxy)]-*p*-phenylene-vinylene (MDMO-PPV) was used as the electron donor²¹ while the electron acceptor was [6,6]-phenyl C₆₁-butyric acid methyl ester (PCBM).²² The enhanced solubility of PCBM compared to C₆₀ allows a high fullerene/conjugated polymer ratio and strongly supports the formation of bulk donor-acceptor heterojunctions. The thickness of the spin-cast MDMO-PPV:PCBM active layer was about 100 nm. As electrodes, a transparent indium-tin-oxide (ITO) film on one side and a LiF/Al bilayer contact on the other side were used. A LiF/Al electrode was chosen instead of pristine Al in order to guarantee a good ohmic contact between the metal and the organic layer.^{23,24} For improvement of the ITO contact, the ITO was coated with a thin layer of poly(ethylene dioxythiophene) (PEDOT).²⁵ The device structure of ITO/PEDOT/MDMO-PPV:PCBM/LiF/Al layered solar cells together with the molecular structure of the compounds used for the active layer are shown in Fig. 1.

In order to permit transportation outside the laboratory where they were produced, the devices had to be protected from oxygen by encapsulation. In an only partially successful attempt to effect such protection, the solar cells were

sandwiched between two glass microscope slides and sealed by epoxy.

Under test the samples were illuminated through their semitransparent ITO/substrate side. The cell temperature, during both simulator and natural sunlight tests, was controlled by a thermoelectric cooling plate upon which the cell was mounted.

In Linz, preliminary indoor photovoltaic measurements of the as-prepared cells were carried out, using a solar simulator, both before and after encapsulation.

In Sede Boqer, the outdoor current-voltage measurements were performed on cloudless days, during the noon-time period, at normal incidence to the incoming solar beam radiation. The solar irradiance, measured with a calibrated thermopile pyranometer (Eppley PSP), was found to remain constant, during the test runs, to within approximately $\pm 0.3\%$ at levels that slightly exceeded 1000 W/m^2 .¹⁹ Moreover, under such conditions, the natural sunlight spectrum at Sede Boqer is known to be exceedingly close to the standard AM1.5G spectrum.²⁰

Because the outdoor solar irradiance level was not, in general, precisely equal to 1000 W/m^2 , it was necessary to adjust the measured values of short-circuit current, I_{sc} , current at the maximum power point, I_{mpp} , and maximum output electrical power, P_{out} , to the STC irradiance value. For conventional inorganic solar cells, the current versus irradiance dependence is known to be linear, but for the novel cells studied here, this fact had to be checked. To do this, we used a solar simulator (also a Steuernagel Solar Constant 575) employing a filtered metal-halide lamp, and wire masks to vary the intensity in the range $80\text{--}550 \text{ W/m}^2$, without changing the spectral quality of the light. This latter point is important because the simulator spectrum is already only an approximation to true AM1.5 so it was important not to introduce further uncertainties by allowing its spectrum to change with changing light intensity. Under these circumstances, it was reasoned, if the cell current turns out to be linear to changes in the intensity of the simulator lamp then in all probability it is safe to assume that it would remain linear under true AM1.5 conditions—particularly for small departures from 1000 W/m^2 . Figure 2 shows a plot of I_{sc} vs simulator light intensity level, at a variety of fixed temperatures in the range $10\text{--}33 \text{ }^\circ\text{C}$. These curves are sufficiently linear to give us confidence that no substantial errors would be introduced into our results by adjusting measurements performed at, say, 1050 W/m^2 , to the standard 1000 W/m^2 level.

The power conversion efficiency η of solar cells under illumination was calculated by

$$\eta = \frac{P_{out}}{P_{in}} = \text{FF} \frac{V_{oc} I_{sc}}{P_{in}}, \quad (1)$$

where P_{out} is the maximum output electrical power of the device under illumination and P_{in} is the light intensity incident on the device, V_{oc} is the open-circuit voltage, I_{sc} is the short-circuit current. FF, the fill factor is given by

$$\text{FF} = \frac{V_{mpp} I_{mpp}}{V_{oc} I_{sc}}, \quad (2)$$

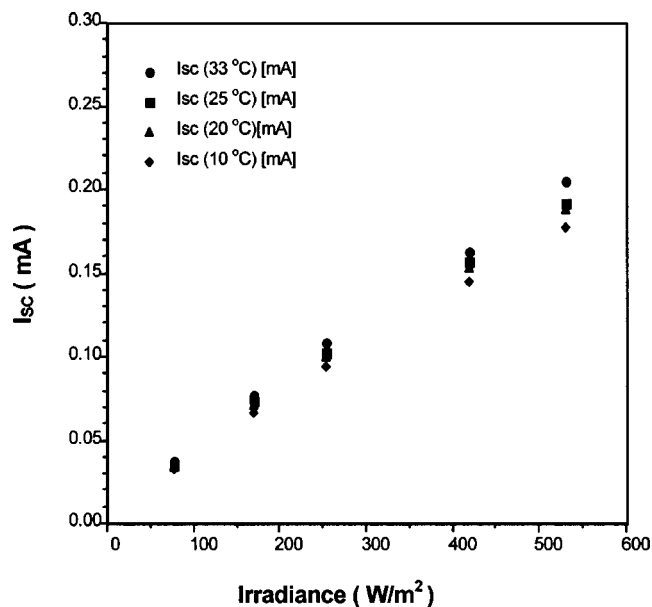


FIG. 2. Short-circuit current (I_{sc}) vs irradiance level of solar simulator (Steuernagel solar constant 575), at various cell temperatures, for a typical cell sample.

where V_{mpp} and I_{mpp} are the voltage and current at the maximum power point, respectively.

Accurate indoor photovoltaic measurements under STC employ a solar simulator, with a light spectrum that approximates the AM1.5 global spectrum and a calibrated reference cell to set the intensity. These measurements can be divided into two steps: (a) the determination of the simulator spectral mismatch factor M ; (b) measurements of the $I-V$ curve of the solar cell and correction to STC.

The match between a simulator spectrum, $E_S(\lambda)$, and the AM1.5G reference spectrum, $E_R(\lambda)$, is never perfect, even for the best solar simulators. Furthermore, a spectral mismatch is introduced since the spectral responses of the device under test, $S_T(\lambda)$, and of the reference cell, $S_R(\lambda)$, are, in general, not identical. In order to correct for this, a spectral mismatch factor M can be computed via the following formula:

$$M = \frac{\int E_R(\lambda) S_R(\lambda) \partial\lambda}{\int E_S(\lambda) S_R(\lambda) \partial\lambda} * \frac{\int E_S(\lambda) S_T(\lambda) \partial\lambda}{\int E_R(\lambda) S_T(\lambda) \partial\lambda}, \quad (3)$$

where each integral in Eq. (3) is proportional to the short-circuit current that would be produced, at standard temperature, by the cell of stated spectral sensitivity $S_i(\lambda)$ under the specified spectrum $E_j(\lambda)$.

For crystalline silicon solar cells, M usually lies in the range 0.98–1.02, since stable calibrated solar cells can be constructed from more-or-less the same material as the test cell. However, for the novel type of solar cells under the present study, suitable and stable reference cells cannot be fabricated yet. This implies that for the measurement of these cells, one has to use calibrated reference cells with a different spectral response from the device under test, resulting in mismatch factors significantly deviating from 1. Therefore, step (a) is the measurement of the spectral sensitivity functions of the reference cell and the test cell, and measurement

TABLE I. Photovoltaic parameters of conjugated polymer-fullerene solar cells measured under simulated AM1.5 conditions before sealing. Measurements were performed with a solar simulator (Steuernagel Solar Constant 575) at an irradiance level of 800 W/m² and a cell temperature of 55 °C. Measured data were corrected to the plotted AM1.5 values using a calculated (see Ref. 17) mismatch factor of 0.76.

	V_{oc} (mV)	J_{sc} (mA/cm ²)	FF	Efficiency (%)	Area (mm ²)
Cell 26	856	3.85	0.598	2.47	6.75
	839	3.9	0.601	2.45	6.9
	837	3.92	0.598	2.46	7.05
Cell 40	858	4.02	0.567	2.46	6.3
	845	3.99	0.585	2.47	6.2
	844	3.90	0.606	2.49	6.15

of the spectrum of the simulator. These measurements, together with the defined spectrum AM1.5G enable M to be calculated. It is of utmost importance to carry out the procedure as precisely as possible in order to minimize measurement errors.

In Petten, the solar cell spectral responses were measured according to the ASTM E1021-84 norm. The cells were illuminated using light from the simulator’s xenon lamp, after passing it through a band filter (20 nm width) and through a chopper, creating “monochromatic” modulated light. White light (1000 W/m²), using halogen lamps, was applied as bias light to create standard measuring conditions.²⁶ A monocrystalline silicon solar cell+KG5 filter calibrated at ISE was used as the reference cell. The spectral response of an encapsulated ITO/PEDOT/MDMO-PPV:PCBM/LiF/Al device was measured relative to the spectral response of the reference cell. Together with the spectral distribution for AM1.5G and the simulator spectrum, a mismatch factor of 0.9 was calculated using Eq. (3). The value $M=0.9$ was then used, in step (b), to correct the measured I_{sc} values of the polymer-fullerene cell to I_{sc} values appropriate to AM1.5G conditions. $I-V$ curves were measured at various cell temperatures in the wide range of the possible operating conditions (25–60 °C) and η and FF were calculated according to Eqs. (1) and (2).

III. RESULTS AND DISCUSSION

Table I summarizes the results of preliminary photovoltaic characterization of solar cells in Linz, directly after production in inert box conditions. Current–voltage measurements were performed under irradiation by a metal-halide solar simulator at light intensity of 800 W/m² and a cell temperature of 55 °C. $I-V$ curves for a typical cell before and after sealing are plotted in Fig. 3. Table I shows that for the various solar cells with active areas in the range (6.15–7.05) mm², the short-circuit current densities were found to be $J_{sc}=(3.85-4.02)$ mA/cm² and, the corresponding open-circuit voltages, fill factors, and energy conversion efficiencies were in the respective ranges: $V_{oc}=(837-858)$ mV, $FF=(0.567-0.606)$, and $\eta=(2.45-2.49)\%$.

After sealing these devices in the manner described above, they were delivered to the partner laboratories where they were subjected to outdoor $I-V$ measurements (in Sede

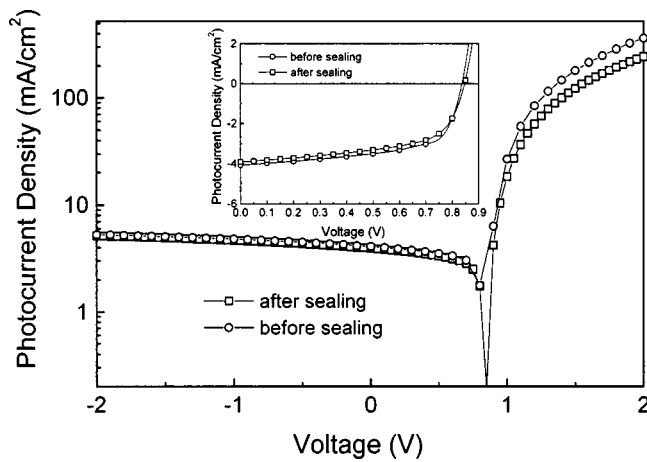


FIG. 3. Typical I - V curves for an "as-produced" polymer-fullerene solar cell before and after sealing. Measurements were performed with a solar simulator (Steuernagel solar constant 575) at an irradiance level of 800 W/m^2 and a cell temperature of 55°C . Measured data were corrected to the plotted AM1.5 values using a calculated (Ref. 17) mismatch factor of 0.76.

Boqer) and indoor measurements (in Petten), at a variety of cell temperatures. Generally, a qualitatively similar temperature behavior was observed by the indoor and outdoor I - V measurements of all devices studied. Figures 4 and 5 summarize the temperature dependencies of the principal cell parameters (V_{oc} , J_{sc} , η , and FF) derived from the outdoor and indoor I - V measurements of typical devices.

Outdoor and simulator measurements of V_{oc} show a linear decrease with increasing temperature [Figs. 4(b) and 5]. Additional outdoor measurements of V_{oc} made while continuously varying the cell temperature, without recording the entire I - V curve confirmed this behavior (Fig. 6). For all samples, the observed linear decrease had a temperature coefficient in the range $dV_{oc}/dT = -(1.40-1.65) \text{ mV/K}$. This is comparable to corresponding values observed for familiar inorganic solar cells in this temperature range. Recent low temperature measurements on the current-voltage behavior of conjugated polymer/fullerene bulk heterojunction solar cells in the range (80–300) K showed that this linear temperature dependence of V_{oc} is lost at temperatures below 200 K and that V_{oc} begins to saturate.²⁷ Nevertheless, we have used the linear temperature coefficient, obtained from the present measurements, extrapolated to $T=0 \text{ K}$ (inset in Fig. 6), in order to derive an upper limit for the value of the open circuit voltage at 0 K. The result is $V_{oc}(0 \text{ K}) = (1.33-1.40) \text{ V}$.

In order to try and understand the physical mechanisms which may be responsible for the observed temperature dependence of V_{oc} in the high and low temperature ranges it is instructive to start with an analysis of the V_{oc} behavior of conventional inorganic semiconductor solar cells with a p - n junction.²⁸ For that situation:

$$V_{oc} = \frac{A \kappa T}{q} \ln \left(\frac{I_{sc}}{I_o} + 1 \right), \quad (4)$$

where A is a so-called diode quality factor of the p - n junction and I_o is the reverse saturation current. According to a geometrically simple model of Shockley,²⁹ I_o is given by

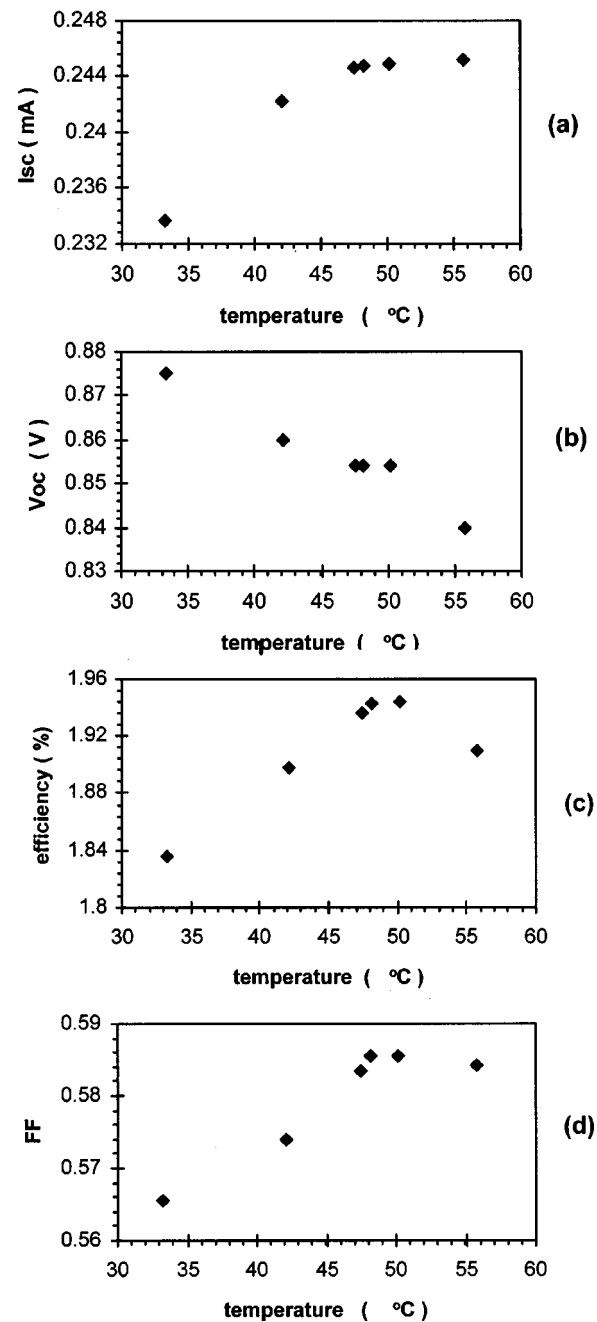


FIG. 4. Temperature dependencies of the principal photovoltaic parameters for a typical polymer-fullerene solar cell derived from outdoor measurements of its I - V curves. Plotted values of efficiency and I_{sc} have been adjusted to the STC irradiance level of 1000 W/m^2 .

$$I_o = q N_v N_c [\exp(-E_g/\kappa T)] \cdot \left(\frac{L_n}{n_n \tau_n} + \frac{L_p}{p_p \tau_p} \right), \quad (5)$$

where N_v and N_c are the effective densities of states in the valence and conduction band, respectively, E_g is the semiconductor band gap, $L_n, L_p, n_n, p_p, \tau_n, \tau_p$ are the diffusion lengths, the carrier densities and the lifetimes of electrons and holes, respectively. Since $I_{sc} \gg I_o$, by inserting Eq. (5) into (4) we obtain:

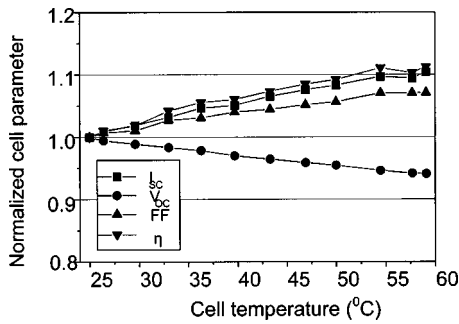


FIG. 5. Temperature dependence of normalized photovoltaic parameters for a typical polymer-fullerene solar cell derived from indoor measurements of its I - V curves. Ordinate axis displays all parameters normalized to their measured values at 25 °C: namely, $J_{sc}=3.1$ mA/cm², $V_{oc}=840$ mV, $FF=0.55$, and $\eta=1.45\%$. Active cell area=7.5 mm². Measurements were performed with a class A solar simulator (Spectrolab X-10). Measured data were corrected to their corresponding AM1.5 values using a mismatch factor of 0.9.

$$V_{oc} = \frac{AE_g}{q} - \frac{A\kappa T}{q} \ln \left[\frac{1}{I_{sc}} \cdot qN_v N_c \right] \left(\frac{L_n}{n_n \tau_n} + \frac{L_p}{p_p \tau_p} \right) = a - bT, \tag{6}$$

where

$$a = V_{oc}(0 \text{ K}) = \frac{AE_g}{q},$$

and

$$b = -dV_{oc}/dT = \frac{A\kappa}{q} \ln \left[\frac{1}{I_{sc}} \cdot qN_v N_c \right] \left(\frac{L_n}{n_n \tau_n} + \frac{L_p}{p_p \tau_p} \right).$$

To the extent to which such a simple model might also be relevant to our organic solar cell situation, i.e., in that we also observe a linear decrease of V_{oc} with T , at least for the high temperature range ($T > 200$ K) – V_{oc} for these solar cells may be described by a diode equation similar to Eq. (4) with $I_o \sim \exp(-E_{DA}/kT)$. Here E_{DA} is a parameter analogous to E_g for a conventional semiconductor. If we adopt such a model for these conjugated polymer-fullerene bulk hetero-

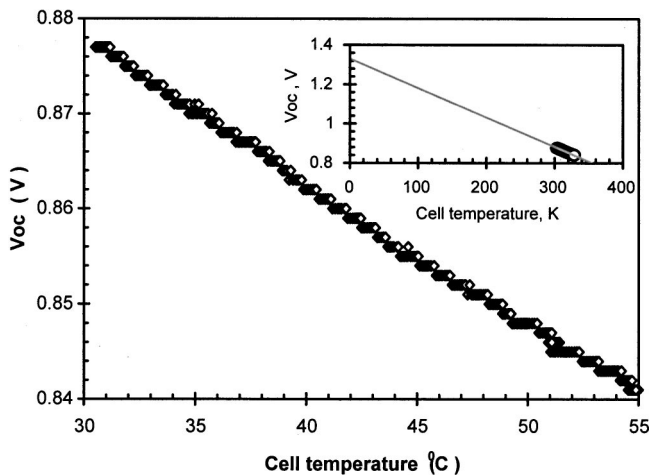


FIG. 6. Outdoor measurement of V_{oc} vs temperature made by continuously varying the cell temperature. Inset shows same data extrapolated to 0 K.

junction solar cells E_{DA} corresponds to the energy difference between the HOMO level of the donor and the LUMO level of the acceptor components of the active layer, as will be argued below. It is important to remark, however, that since our experiments have been performed over a relatively small range of temperatures, we can not rule out a possible temperature dependence of E_{DA} for temperatures substantially different from the range investigated.

Our observation of a V_{oc} of ~ 0.8 V is considerably higher than the V_{oc} value of 0.53 V previously reported for bilayer conjugated polymer/fullerene solar cells.⁹ This result strongly supports the conclusion of Ref. 11 that photovoltage generation in bulk donor-acceptor heterojunctions cannot be explained by a model of the work function difference of the two electrodes³⁰ (which is generally accepted for single layer conjugated polymers devices,^{31,32} or by a picture involving only band bending at the polymer/fullerene interface (which is adequate for bilayer conjugated polymer-fullerene solar cells with nonrectifying metal contacts¹⁰).

On the other hand, it has recently been shown that the open-circuit voltage in solar cells based on interpenetrating networks of conjugated polymers with fullerenes is directly related to the acceptor strength of the fullerenes.³³ This result fully supports the view that the open-circuit voltage of this type of donor-acceptor bulk-heterojunction cell is related directly to the energy difference between the HOMO level of the donor and the LUMO level of the acceptor components of the active layer. Furthermore, and also in full agreement with this view, it was found that a variation of the negative electrode work function influences the open-circuit voltage only in a minor way. In accord with results from XPS studies proving the existence of surface charges on C₆₀ at metal interfaces, this electrode-insensitive voltage behavior was identified as a result of Fermi level pinning between the negative metal electrode and the fullerene reduction potential via charged interfacial states.³³ This view on the V_{oc} generation is additionally supported by the fact that the values of temperature coefficient $dV_{oc}/dT = -(1.40-1.65)$ mV/K for the cells under the present study (with bilayer LiF/Al and ITO/PEDOT contacts) coincide with those we reported for polymer/fullerene bulk heterojunction solar cells of the “previous generation” (i.e., with the same components in the active layer but without LiF and PEDOT contact layers).³⁴

From the results presented in Ref. 33 the following equation for the open circuit voltage in the donor/acceptor bulk heterojunction solar cells was proposed:

$$V_{oc} = (A_{ox} - S_1 \times E_{red(A)}) - S_2 \times (\phi_M - E_{red(A)}) + C. \tag{7}$$

Here ϕ_M is the work function of the metal and C is a constant describing the interface potential for the ideal ohmic contact. $E_{red(A)}$ is the reduction potential of the acceptor (PCBM in our case), which is representative for the Fermi level of the acceptor under illumination. A_{ox} is a constant representative of all the contributions to V_{oc} from the positive electrode, and is expected to be properly described by the oxidation potential of the conjugated polymer. S_1 and S_2 are a quality factor for the ohmicity of this contact and the index of interface behavior,³⁵ respectively. For the bulk heterojunction solar cells presented in this work, S_1 was found

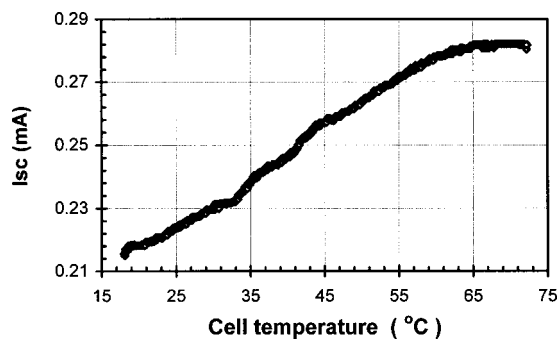


FIG. 7. Outdoor measurement of I_{sc} vs temperature made by continuously varying the cell temperature. Plotted values have been adjusted to the STC irradiance level of 1000 W/m^2 .

to be close to 1 while S_2 was found to be around 0.1. A similar dependence of V_{oc} on the Fermi level of the illuminated polymer (properly described by the oxidation potential of the polymer) is expected, and work is in progression to investigate this dependence.

In this image, the temperature dependence of V_{oc} is directly correlated to the temperature dependence of the quasi-Fermi levels of the components of the active layer under illumination, i.e., of the polymer and the fullerene. Therefore, knowledge of the temperature dependence of V_{oc} over a wide range, and especially $V_{oc}(0 \text{ K})$, is essential for the understanding of bulk heterojunction solar cells.

Figures 4(a), 4(d), and 5 show relatively large monotonic increase with temperature for I_{sc} and FF, followed by a saturation region. A slight increase in I_{sc} with temperature is also a common feature for inorganic solar cells.³⁶ However, in the case of our polymer-fullerene solar cells the rate of increase is so dramatic that the increase of the short-circuit current-fill factor product with temperature overtakes the decrease of open-circuit voltage with temperature. As a result, there is an absolute increase of the power efficiency η with temperature, reaching a maximum value at temperature T_{max} which, for different samples, lies in the range $47\text{--}60^\circ\text{C}$ [Figs. 4(c) and 5].

In order to investigate this behavior more thoroughly we measured I_{sc} with continuous variation of the cell temperature, without recording the entire $I\text{--}V$ curve. The result is shown in Fig. 7 (for another sample), where a clear indication of saturation sets in at around 60°C . This, together with the continued falloff in V_{oc} , would result in a subsequent decrease in the efficiency with further increase in temperature. A noteworthy point, which provides further confirmation of this result, is that when the cell temperature was cycled back and forth there was no hysteresis in the I_{sc} temperature dependence.

Solar cells based on interpenetrating networks of conjugated polymers with fullerenes are known to be sensitive to the combination of oxygen and light. Unprotected devices show rapid degradation under light/air exposure.³⁷ Due to this degradation process and to the imperfect encapsulation process employed for the present cells, it is difficult to make quantitative comparisons among the results of photovoltaic characterization of the cells at different stages of their degradation. In particular, it is meaningless to compare the ab-

solute results of our outdoor and indoor $I\text{--}V$ measurements. However, in addition to qualitative coincidence of the temperature dependencies of the cell parameters observed by the indoor and outdoor $I\text{--}V$ measurements, we may report that after 6 h of irradiation during 11 successive days of the outdoor experiment, absolute values of V_{oc} and its temperature dependence [$dV_{oc}/dT, V_{oc}(0 \text{ K})$] remained almost constant. On the other hand, degradation was evident in the absolute values of I_{sc} and FF, while the positive trend in the temperature dependencies of I_{sc} , FF, and η was not influenced.

A positive temperature dependence of η is a remarkable peculiarity for solar cells, which is not observed in most conventional inorganic solar cells.³⁶ It is significant, therefore, that the heating of solar cells to temperatures in the range of our T_{max} may be expected to arise naturally by the absorption of solar radiation, i.e., without any artificial heating. Therefore, unlike conventional solar cells, we would expect polymer-fullerene solar cells to perform more efficiently under natural (warm climate) operating conditions than under standard test conditions!

Very recently it was demonstrated theoretically and experimentally that I_{sc} in conjugated polymer-fullerene solar cells is controlled to a considerable extent by mobility of the majority charge carriers in the cell's active layer.³⁸ Moreover, expressed activated behavior of charge carrier mobility in conjugated polymers is known to result in higher mobility at higher temperatures (for review see Ref. 39). Accordingly, it is likely that our observed, unusually large, positive temperature coefficient for I_{sc} originates from the temperature dependence of the mobility of the conjugated polymer-fullerene composite.

This hypothesis is also in accord with our irradiance-resolved measurements performed at different cell temperatures using the solar simulator (Fig. 2). In those measurements we observed a linear increase of I_{sc} , with light intensity for the whole range of irradiance and temperature, but we may also draw attention to the fact that the slope of the irradiance dependence of I_{sc} increases with increasing temperature. In other words, the maximum temperature influence is observed at the highest light intensities. At such intensities a maximum amount of photocarriers are generated and the limitation in carrier transport, caused by the low mobility of holes in the conjugated polymer and electrons in the fullerene channels, is more evident than for lower carrier densities.

The observed temperature dependence of FF [Figs. 4(d) and 5] is quite similar to that of I_{sc} . The former, however, can be qualitatively understood in terms of the temperature-dependent series resistance of the solar cell, R_s , as the following argument demonstrates. With familiar inorganic solar cells the series resistance is determined principally by the contacts and contact/semiconductor interfaces, because the resistivity of the semiconductor material is relatively low. On the other hand, our plastic solar cells have a relatively high resistivity of the organic active layer but one which *decreases* with increasing temperature owing to the increase in carrier mobility. It is this decrease in resistivity that manifests itself as an improvement in the fill factor with increased temperature.

Recently, we reported a similar temperature dependence of I_{sc} , V_{oc} , and η for a “previous generation” of solar cells based on interpenetrating networks of conjugated polymers with fullerenes (with initial efficiency $\leq 1\%$).³⁴ We have also observed a positive temperature coefficient for the efficiency of C_{60} single-crystal photoelectrochemical cells.⁴⁰ Furthermore, although not explicitly stated by the authors, one may also find indications for such an effect in data recently published on organic (magnesium phthalocyanine)/inorganic (silicon) heterojunction solar cells.⁴¹ Finally, a temperature dependence of I_{sc} qualitatively similar to that shown in Figs. 4(a), 5, and 7 was also observed for organic solar cells based on Zn-phthalocyanine (ZnPc)/perylene (M-PP) heterojunction.⁴² We suggest that positive temperature dependencies of I_{sc} , FF, and η may be characteristic for solar cells with an expressed temperature activated behavior for charge transport, resulting in higher mobility/conductivity at higher temperatures (for example, for some types of amorphous silicon solar cells⁴³).

In organic semiconductors, the nature of charge transport, in particular, the character of the temperature dependence of mobility is known to depend strongly upon their crystalline structure. For example, it was found that the activation energy for mobility decreases with increasing grain size in polycrystalline small molecule samples.⁴⁴ Furthermore, in high quality single crystals of pentacene the mobility of electrons and holes was even found to decrease with increasing temperature following a power law familiar for inorganic semiconductors.⁴⁵ It is significant that solar cells based on such single crystals⁸ demonstrate a conventional negative temperature coefficient for their efficiency.⁴⁶ This fact provides additional support to our hypothesis on the relationship between the temperature dependence of mobility and that of I_{sc} , FF, and η .

IV. CONCLUSIONS

We have investigated the temperature dependence of photovoltaic parameters for solar cells based on interpenetrating networks of conjugated polymers with fullerenes. The open-circuit voltage, V_{oc} , of these cells was found to decrease linearly with increasing temperature, with a temperature coefficient dV_{oc}/dT in the range $-(1.40-1.65)$ mV/K in the temperature regime between 10 and 60 °C. We observed a monotonic increase in temperature for the short-circuit current and the fill factor, followed by a saturation region. For the temperature range under investigation it was found that the increase in the current-fill factor product can overtake the decrease of voltage with temperature and result in an overall increase of the energy conversion efficiency with increasing temperature, which reaches its maximum value in the range 47–60 °C. We have argued that this behavior originates from the temperature dependence of the mobility in the conjugated polymer-fullerene composite due to thermal activation of its charge carrier mobility. We suggest that positive temperature dependencies of short-circuit current and efficiency may be characteristic for other kinds of solar cells with thermal activation of their charge transport.

ACKNOWLEDGMENTS

This work was funded in part by the European Community DG XII under Contract No. JOR3-CT-98-0206 (DG 12-WSMN). E.A.K. acknowledges financial support from the Israel Ministry of Immigrant Absorption and from the Genseler Foundation. S.M.T. wishes to thank the Albert Katz International School for Desert Studies and the Bonna Terra Foundation for support. Part of this work was performed within the Christian Doppler Society’s dedicated laboratory on Plastic Solar Cells funded by the Austrian Ministry of Economic Affairs and Quantum Solar Energy Linz Ges. M.B.H. The work was further supported by the “Fonds zur Förderung der Wissenschaftlichen Forschung” of Austria (Project No. P-12680-CHE) and by the Land Oberösterreich (ETP).

- ¹J. D. Wright, *Molecular Crystals* (Cambridge University Press, Cambridge, UK, 1995).
- ²M. Kaneko, in *Handbook of Organic Conductive Molecules and Polymers*, edited by H. S. Nalwa (Wiley, New York, 1997), Vol. 4, p. 661.
- ³C. W. Tang, *Appl. Phys. Lett.* **48**, 183 (1986).
- ⁴D. Wöhrle and D. Meissner, *Adv. Mater.* **3**, 129 (1991).
- ⁵J. J. M. Halls, C. A. Walsh, N. C. Greenham, E. A. Marseglia, R. H. Friend, S. C. Moratti, and A. B. Holmes, *Nature (London)* **376**, 498 (1995).
- ⁶M. Granström, K. Petritsch, A. C. Arias, A. Lux, M. R. Anderson, and R. H. Friend, *Nature (London)* **395**, 257 (1998).
- ⁷P. Peumans, V. Bulovich, and S. R. Forrest, *Appl. Phys. Lett.* **76**, 2650 (2000).
- ⁸J. H. Schön, Ch. Kloc, E. Buher, and B. Batlogg, *Nature (London)* **403**, 408 (2000).
- ⁹N. S. Sariciftci, D. Braun, C. Zhang, V. I. Srdanov, A. J. Heeger, G. Stucky, and F. Wudl, *Appl. Phys. Lett.* **62**, 585 (1993).
- ¹⁰G. Yu, J. Gao, J. C. Hummelen, F. Wudl, and A. J. Heeger, *Science* **270**, 1789 (1995).
- ¹¹C. J. Brabec, F. Padinger, N. S. Sariciftci, and J. C. Hummelen, *J. Appl. Phys.* **85**, 6866 (1999).
- ¹²D. Gebeyehu, C. J. Brabec, F. Padinger, T. Fromherz, J. C. Hummelen, D. Badt, H. Schindler, and N. S. Sariciftci, *Synth. Met.* **118**, 1 (2001).
- ¹³N. S. Sariciftci and A. J. Heeger, in *Handbook of Organic Conductive Molecules and Polymers*, edited by H. S. Nalwa (Wiley, New York, 1997), Vol. 1, p. 413.
- ¹⁴N. S. Sariciftci, L. Smilowitz, A. J. Heeger, and F. Wudl, *Science* **258**, 1474 (1992).
- ¹⁵L. Smilowitz, N. S. Sariciftci, R. Wu, C. Gettinger, A. J. Heeger, and F. Wudl, *Phys. Rev. B* **47**, 13835 (1993).
- ¹⁶C. J. Brabec, G. Zerza and N. S. Sariciftci, G. Cerullo, S. DeSilvestri, S. Luzatti, and J. C. Hummelen, *Chem. Phys. Lett.* (in press).
- ¹⁷S. E. Shaheen, C. J. Brabec, N. S. Sariciftci, F. Padinger, T. Fromherz, and J. C. Hummelen, *Appl. Phys. Lett.* **78**, 841 (2001).
- ¹⁸J. Rostalski and D. Meissner, *Sol. Energy Mater. Sol. Cells* **21**, 87 (2000).
- ¹⁹D. Berman, S. Biryukov, and D. Faiman, *Sol. Energy Mater. Sol. Cells* **36**, 421 (1995).
- ²⁰D. Berman and D. Faiman, *Sol. Energy Mater. Sol. Cells* **45**, 401 (1997).
- ²¹G. H. Gelinck, J. Warman, and E. G. J. Staring, *J. Phys. Chem.* **100**, 5485 (1996).
- ²²J. C. Hummelen, B. W. Knight, F. Lepec, and F. Wudl, *J. Org. Chem.* **60**, 532 (1995).
- ²³G. E. Jabbour, B. Kippelen, N. R. Armstrong, and N. Peyghambarian, *Appl. Phys. Lett.* **73**, 1185 (1998).
- ²⁴L. S. Hung, C. W. Tang, and M. G. Mason, *Appl. Phys. Lett.* **70**, 152 (1997).
- ²⁵T. Fromherz, F. Padinger, D. Gebeyehu, C. J. Brabec, J. C. Hummelen, and N. S. Sariciftci, *Sol. Energy Mater. Sol. Cells* **63**, 61 (2000).
- ²⁶P. M. Sommeling, H. C. Rieffe, J. A. M. van Roosmalen, A. Schönecker, J. M. Kroon, J. A. Wienke, and A. Hinsch, *Sol. Energy Mater. Sol. Cells* **62**, 399 (2000).
- ²⁷V. Dyakonov, I. Riedel, J. Parisi, C. J. Brabec, N. S. Sariciftci, and J. C.

- Hummelen, in *Proceedings of the 13th International Workshop on Quantum Solar Energy Conversion*, March 10–17, Kirchberg/Tirol, 2001 (in press).
- ²⁸A. L. Fahrenbruch and R. H. Bube, *Fundamentals of Solar Cells, Photovoltaic Solar Energy Conversion* (Academic, New York, 1983).
- ²⁹W. Shockley, *Electrons and Holes in Semiconductors* (Van Nostrand, New York, 1950).
- ³⁰I. D. Parker, *J. Appl. Phys.* **75**, 1656 (1994).
- ³¹G. Yu and A. J. Heeger, *J. Appl. Phys.* **78**, 4510 (1995).
- ³²G. Yu, C. Zhang, and A. J. Heeger, *Appl. Phys. Lett.* **64**, 1540 (1994).
- ³³C. J. Brabec, A. Cravino, T. Fromherz, D. Meissner, N. S. Sariciftci, J. C. Hummelen, M. T. Rispens, L. Sanchez, and J. C. Hummelen, *Adv. Funct. Mater.* (submitted).
- ³⁴E. A. Katz, D. Faiman, Y. Cohen, F. Padinger, C. Brabec, and N. S. Sariciftci, *Proc. SPIE* **4108**, 117 (2001).
- ³⁵L. J. Brillson, *Surf. Sci. Rep.* **2**, 145 (1982).
- ³⁶K. Emery, J. Burdick, Y. Caiyem, D. Dunlavy, H. Field, B. Kroposki, T. Moriarty, L. Ottoson, S. Rummel, T. Strand, and M. W. Wanlass, in *Proceedings of the 25th IEEE Photovoltaic Spec. Conference* (IEEE, 1996), p. 1275.
- ³⁷H. Neugebauer, C. Brabec, J. C. Hummelen, and N. S. Sariciftci, *Sol. Energy Mater. Sol. Cells* **61**, 35 (2000).
- ³⁸C. J. Brabec, S. E. Shaheen, T. Fromherz, F. Padinger, J. C. Hummelen, A. Dhanabalan, R. A. J. Janssen, and N. S. Sariciftci, *Synth. Met.* **1517–1521**, 121 (2001).
- ³⁹P. W. M. Blom and M. C. J. M. Vissenberg, *Mater. Sci. Eng., R.* **27**, 53 (2000).
- ⁴⁰S. Licht, P. A. Ramakrishnan, D. Faiman, E. A. Katz, A. Shames, and S. Goren, *Sol. Energy Mater. Sol. Cells* **56**, 45 (1998).
- ⁴¹S. Riad, *Thin Solid Films* **370**, 253 (2000).
- ⁴²S. Günster, S. Siebentritt, and D. Meissner, *Mol. Cryst. Liq. Cryst.* **229**, 111 (1993).
- ⁴³D. Faiman (unpublished).
- ⁴⁴G. Horowitz and M. E. Hajlaoui, *Adv. Mater.* **12**, 1046 (2000).
- ⁴⁵J. H. Schön, S. Berg, Ch. Kloc, and B. Batlogg, *Science* **287**, 1022 (2000).
- ⁴⁶J. H. Schön (private communication).